

# Searches for additional Higgs bosons decaying to tau leptons at the LHC

C. Caputo<sup>1</sup>,

on behalf of the *ATLAS* and *CMS* collaborations.

<sup>1</sup> Centre for Cosmology, Particle Physics and Phenomenology,  
 Université catholique de Louvain, Louvain-la-Neuve B-1348, Belgium

\* claudio.caputo@cern.ch

December 21, 2018



*Proceedings for the 15th International Workshop on Tau Lepton Physics,  
 Amsterdam, The Netherlands, 24-28 September 2018*

scipost.org/SciPostPhysProc.Tau2018

## Abstract

The searches for additional Higgs bosons decaying to tau leptons in scenarios beyond the standard model will be summarised, from the pp collision data collected by the ATLAS and CMS experiments at LHC Run-2.

## Contents

<b>1</b>	<b>Introduction</b>	<b>1</b>
<b>2</b>	<b>Search for a neutral MSSM Higgs boson decaying into <math>\tau\tau</math></b>	<b>2</b>
<b>3</b>	<b>Search for charged Higgs bosons with the <math>H^\pm \rightarrow \tau^\pm\nu</math></b>	<b>6</b>
<b>4</b>	<b>Search for new light bosons in decays of the <math>h(125)</math></b>	<b>9</b>
4.1	$h \rightarrow aa \rightarrow b\bar{b}\tau\tau$	9
4.2	$h \rightarrow aa \rightarrow \mu\mu\tau\tau$	9
4.3	Results	10
<b>5</b>	<b>Conclusion</b>	<b>10</b>
	<b>References</b>	<b>12</b>

## 1 Introduction

The discovery of a new particle in July 2012 by the ATLAS [1] and CMS [2] collaborations at the Large Hadron Collider (LHC) [3] [4, 5], compatible with the standard model (SM) Higgs boson, is a fundamental step forward in our understanding of the electroweak spontaneous symmetry breaking. However, many open questions, including the problem

of the large hierarchy between the Plack and electroweak scale, still need to be addressed. In order to cope with this, many different extension of the SM have been proposed, like supersymmetry (SUSY) [6, 7].

Extending the SM entails, in most of the cases, the extension of the Higgs sector. One of the simple extensions is described by the 2 Higgs Doublet Model (2HDM), where two scalar Higgs doublets are introduced. The spontaneous symmetry breaking give rise to five scalar bosons: a neutral CP-odd  $A$ , two neutral CP-even  $h$  and  $H$ , two charged bosons  $H^\pm$ . In the decoupling limit, the lightest scalar of 2HDM can have properties compatible with discovered Higgs boson; in this scenario all other scalars have larger masses.

Considering how the two doublets can interact with other particles of the SM, different phenomenology scenarios can appear. One of this scenarios is the Type-II 2HDM, which supposes that the first doublet couples only with up-quarks, while the second doublet only with down-quarks and charged fermions.

The Minimal Supersymmetric Standard Model (MSSM) [8, 9], which incorporate the supersymmetry, is a Type-II 2HDM. At tree level, all the phenomenology can be described by two parameters, conventionally chosen to be the mass of the pseudoscalar Higgs  $m_A$  and the ratio between the two vacuum expectation values (VEVs)  $\tan\beta = \nu_1/\nu_2$ .

For  $A$  and  $H$  the dominant production process is still the gluon fusion, for small and medium values of  $\tan\beta$ , followed by the  $b\bar{b}$ -associated production, that increase at high  $\tan\beta$  due to the second doublet couplings to down-type fermions. The  $H^\pm$  production mechanism is strictly connected to the mass of the charged boson. For mass below the top-quark mass ( $m_{H^\pm} < m_t$ ) the decay mode in a  $\tau$  lepton plus is neutrino dominate in a Type-II 2HDM scenario; for mass above the top-quark mass ( $m_{H^\pm} > m_t$ ), decay mode  $\tau\nu$  increase with  $\tan\beta$ . In this report, results of direct searches of MSSM Higgs bosons with tau leptons in the final state, from the ATLAS and CMS collaborations using the 2016 dataset, are presented.

A complex  $SU(2)_L$  singlet field  $S$  can be added to 2HDM, with a small mixing with the doublets; such a model is called 2HDM+S. This leads to two additional singlet states, a CP-odd scalar  $a$  and a CP-even  $s$ , which inherit a mixture of the Higgs doublets fermion interactions. In such a model, also known as NMSSM, the branching fraction of the Higgs boson to a pair of  $a$  or  $s$  bosons can be sizeable, and a wide variety of exotic Higgs decays are allowed [10], especially  $h \rightarrow aa$ . In this report, results of direct searches of  $h \rightarrow aa$  with tau leptons in the final state, from the CMS collaborations using the 2016 dataset, are presented.

## 2 Search for a neutral MSSM Higgs boson decaying into $\tau\tau$

The coupling of the  $H$  and the  $A$  to down-type fermions, at leading-order (LO), is enhanced by  $\tan\beta$  with respect to the expectation for an SM Higgs boson of the same mass, while the coupling to vector bosons and up-type fermions is suppressed. The enhanced coupling to down-type fermions makes searches for additional heavy neutral Higgs bosons that exploit final states containing  $\tau\tau$  particularly interesting. It also has consequences for the production: firstly, the production in association with  $b$  quarks dominates over the production via gluon fusion for large values of  $\tan\beta$ . Secondly, in gluon fusion production the kinematic properties of the Higgs boson change as a function of  $\tan\beta$  due to the increasing contribution of  $b$  quarks in the fermion loop. Diagrams for  $h$ ,  $H$ , and  $A$  production at LO are shown in Figure 1.

The ATLAS and CMS collaborations performed the direct search in the most sensitive final states of the taus [11] [12]. Both focus their attention on  $e\tau_h$ ,  $\mu\tau_h$  and  $\tau_h\tau_h$ , where  $\tau_h$

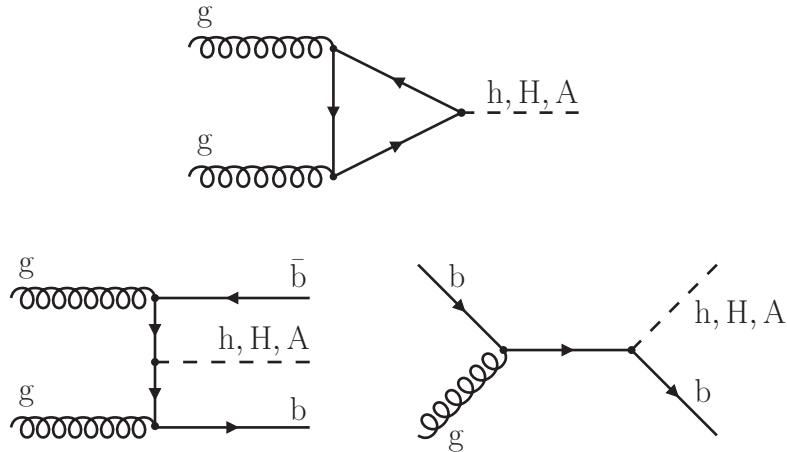


Figure 1: Feynman diagrams of the production modes of a neutral MSSM Higgs boson. (top) Gluon gluon fusion (bottom-left)  $b\bar{b}$ -associated production *four-flavour* scheme (bottom-right)  $b\bar{b}$ -associated production *five-flavour* scheme

79 indicates a tau decaying hadronically; CMS consider also the  $e\mu$  final state. The dataset  
 80 analyzed corresponds to the full statistics available from 2016 collisions,  $\sim 36 \text{ fb}^{-1}$ , at  
 81 center-of-mass energy of 13 TeV. Events are categorized in order to exploit the topological  
 82 kinematic peculiarities of MSSM production mechanisms. The categories depend whether  
 83 a b-jet is found in the event, in order to select the  $b\bar{b}$ -associated production if a b-jet  
 84 is present (b-tag), or select the gluon fusion production if no b-jet is found (b-veto).  
 85 Further sub-categorization are performed to add more control regions used for constraining  
 86 particular backgrounds.

87 The dominant background contribution comes from misidentification of jets as  $\tau_h$ ,  
 88 which is estimated using a data-driven technique called *Fake-Factor Method*. This method  
 89 is extensively explained in [11, 12]. Other important background contributions come from  
 90  $Z/\gamma^* \rightarrow \tau\tau$  production in the b-veto category,  $t\bar{t}$  production in the b-tag category, and  
 91 to a lesser extent  $W(\rightarrow l\nu)$ +jets, single top-quark, diboson and  $Z(\rightarrow ll)$ +jets production.  
 92 These contributions are estimated using simulation, in some cases re-normalized using  
 93 control regions in data. Corrections are applied to the simulation to account for mis-  
 94 modelling of the trigger, reconstruction, identification and isolation efficiency, the electron  
 95 to  $\tau_h^{vis}$  misidentification rate and the momentum scales and resolutions.

The total transverse mass of the system is used as final discriminant to search for an  
 excess due to signal,

$$m_T^{\text{tot}} = \sqrt{m_T^2(\tau_1, \tau_2) + m_T^2(\tau_1, E_T^{\text{miss}}) + m_T^2(\tau_2, E_T^{\text{miss}})},$$

96 where  $\tau_1$  and  $\tau_2$  respectively refer to the  $p_T$  leading and sub-leading taus, while  $E_T^{\text{miss}}$   
 97 is the missing energy measured in the event considered. The  $m_T^{\text{tot}}$  binned distribution is  
 98 fitted simultaneously in all the categories used in the analysis. No evidence for a signal  
 99 is found. Both collaborations set upper limits at 95% confidence level (CL) on the cross-  
 100 section times branching fraction for two dominant production modes, gluon fusion and  
 101  $b\bar{b}$ -associated production. The limits are computed in the narrow width approximation.  
 102 Figure 2 shows the upper limits obtained by the ATLAS and CMS collaborations as a  
 103 function of Higgs boson mass.

104 Results are re-interpreted in two different benchmark scenario models; the  $m_h^{\text{mod}+}$  and  
 105 the hMSSM scenarios [13, 14]. Figure 3 shows limits set on  $m_A - \tan\beta$  plane.

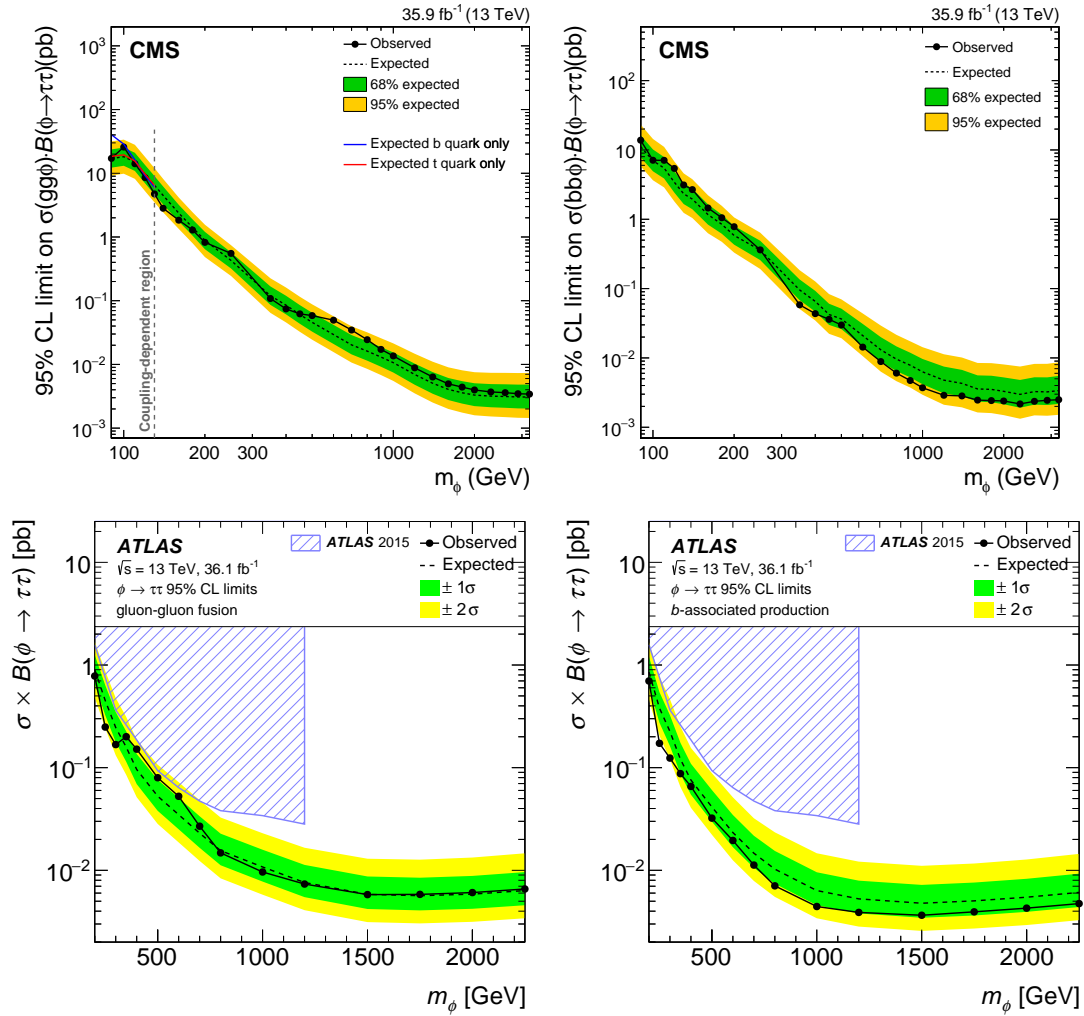


Figure 2: (top) ATLAS expected and observed limits on  $\sigma(\phi) \times BR(\phi \rightarrow \tau\tau)$  for (left) the gluon fusion and (right) the  $b\bar{b}$ -associated production, resulting from the combination of all the three channels considered. (bottom) CMS expected and observed limits on  $\sigma(\phi) \times BR(\phi \rightarrow \tau\tau)$  for (left) the gluon fusion and (right) the  $b\bar{b}$ -associated production, resulting from the combination of all the four channels considered. [11] [12]

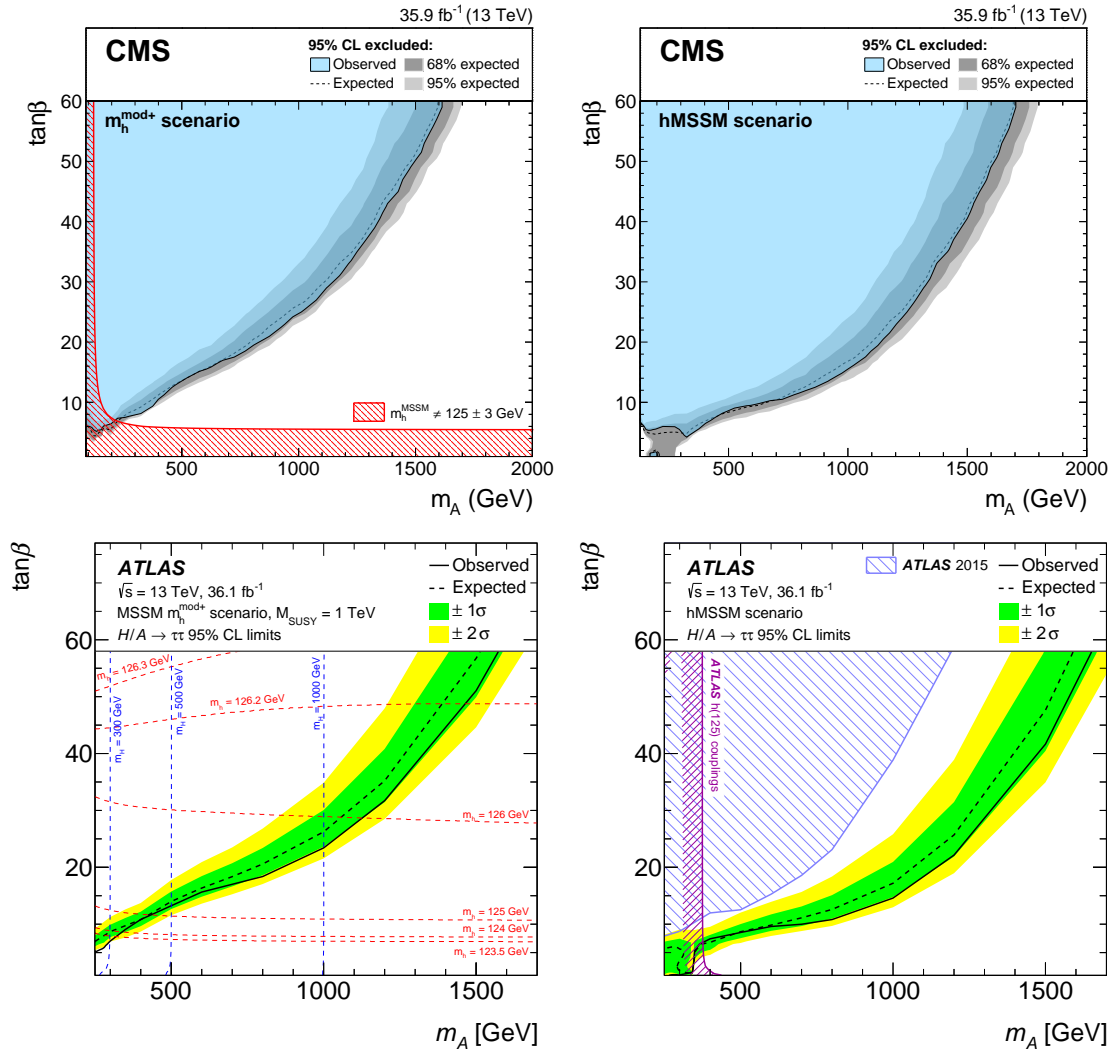


Figure 3: Model dependent exclusion limits in the  $m_A - \tan\beta$  plane for the (left)  $m_h^{\text{mod}+}$  and the (right) hMSSM scenarios. In the top left plot, the red shade area indicates the region that does not give a light  $h$  higgs boson consistent with a mass of 125 GeV within the theoretical uncertainties  $\pm 3$  GeV. In the bottom left plot, the red dashed lines represent the different parameters value that give a particular  $m_h$  value. In the bottom right plot, the purple area indicates the region already excluded by constrains on  $h(125)$  couplings. [11] [12]

### 106 3 Search for charged Higgs bosons with the $H^\pm \rightarrow \tau^\pm \nu$

107 The  $H^\pm$  production mechanism is strictly connected to the mass of the charged boson. If  
 108  $H^\pm$  mass is below the top-quark mass ( $m_{H^\pm} < m_t$ ), the production mode goes through  
 109 the decay of a top-quark,  $t \rightarrow bH^\pm$ , in a  $t\bar{t}$  production. In this mass range, the decay  
 110 mode in a  $\tau$  lepton plus is neutrino dominate in a Type-II 2HDM scenario. If  $H^\pm$  mass  
 111 above the top-quark mass ( $m_{H^\pm} > m_t$ ), the dominant production mode is  $gg \rightarrow tbH^\pm$ .  
 112 In this mass range, the dominant decay is  $H^+ \rightarrow tb$ , considering the alignment limit  
 113 ( $\cos\beta - \alpha \simeq 0$ ) [15]; however the branching fraction for  $H^+ \rightarrow \tau\nu$  can reach up to 10÷15%  
 114 at high  $\tan\beta$ . The mass region where the  $H^\pm$  and the top-quark masses are similar  
 115 ( $m_{H^\pm} \simeq m_t$ ) involves interference effects among the  $t\bar{t}$  and  $H^\pm$  non-resonant top-quark  
 116 productions. Recently theoretical prediction become available for this region [16], which  
 117 now allows to compare directly the  $H^\pm$  model with data in proximity of the top-quark  
 118 mass. In Figure 4 the different production modes Feynman diagrams are depicted.

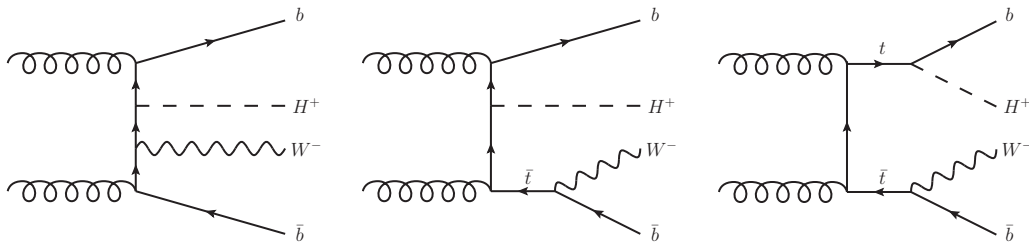


Figure 4: Examples of leading-order Feynman diagrams contributing to the production of charged Higgs bosons in pp collisions: (left) non-resonant top-quark production, (center) single-resonant top-quark production that dominates at large  $H^+$  masses, (right) double-resonant top-quark production that dominates at low  $H^+$  masses. The interference between these three main diagrams becomes most relevant in the intermediate-mass region.

119 The ATLAS and CMS collaboration searched for a charged Higgs boson in pp collision  
 120 using the full 2016 dataset,  $\sim 36 fb^{-1}$ , at a center-of-mass energy of 13 TeV [17] [18]. The  
 121 results presented will refer to the ATLAS search, the only one with the full 2016 dataset  
 122 public at the time of the conference.

123 Two different channels are considered:  $\tau_h$ +jets and  $\tau_h$ +lepton, where both aim to  
 124 different decays of the top-quark produced with the  $H^\pm$ . Furthermore, a multivariate  
 125 discriminant is used to increase the search sensitivity, exploiting the kinematic variables  
 126 that differentiate between signal and backgrounds. The output score of a *Boosted Decision  
 127 Trees* (BDTs) is used as final discriminant. In order to take advantage of the different  
 128  $H^\pm$  decay products' kinematic regime, simulated signal sample are divide in five  $H^\pm$  mass  
 129 bins: 90–120 GeV, 130–160 GeV, 160–180 GeV, 200–400 GeV and 500–2000 GeV. The  
 130 BDTs are trained using a set of variables related to the particular final state.

131 Backgrounds classification and estimation depends on the type of object that gives rise  
 132 to the identified  $\tau_h$ . If  $\tau_h$  arise from a true hadronically decaying tau or electron/muon  
 133 misidentification, simulation is used to estimate such backgrounds like  $Z$ +jets,  $W$ +jets or  
 134 dibosons; however, in the case of  $t\bar{t}$  events, the normalization is obtained from a fit to the  
 135 data. If  $\tau_h$  arise from a misidentified gluon-jet or quark-jet, the *Fake Factor Method* is  
 136 used to estimate such background [17]. Figure 5 shows the BDTs output for the  $\tau_h$ +jets  
 137 final state after estimating the different background contributions.

138 BDTs binned distribution are fitted simultaneously in all the three signal regions. The

139 data are found to be consistent with the background-only hypothesis. Exclusion limits  
 140 are set at 95% CL on  $\sigma(pp \rightarrow tbH^+) \times B(H^+ \rightarrow \tau\nu)$  for the full mass range, as well as  
 141 on  $B(t \rightarrow bH^+) \times B(H^+ \rightarrow \tau\nu)$  for low mass range. Figure 6 shows the expected and  
 142 observed exclusion limits as a function of the  $H^\pm$  mass hypothesis. Figure 7 shows 95%  
 143 CL exclusion limits on  $\tan\beta$  as a function of the charged Higgs boson mass in the context  
 144 of the hMSSM scenario.

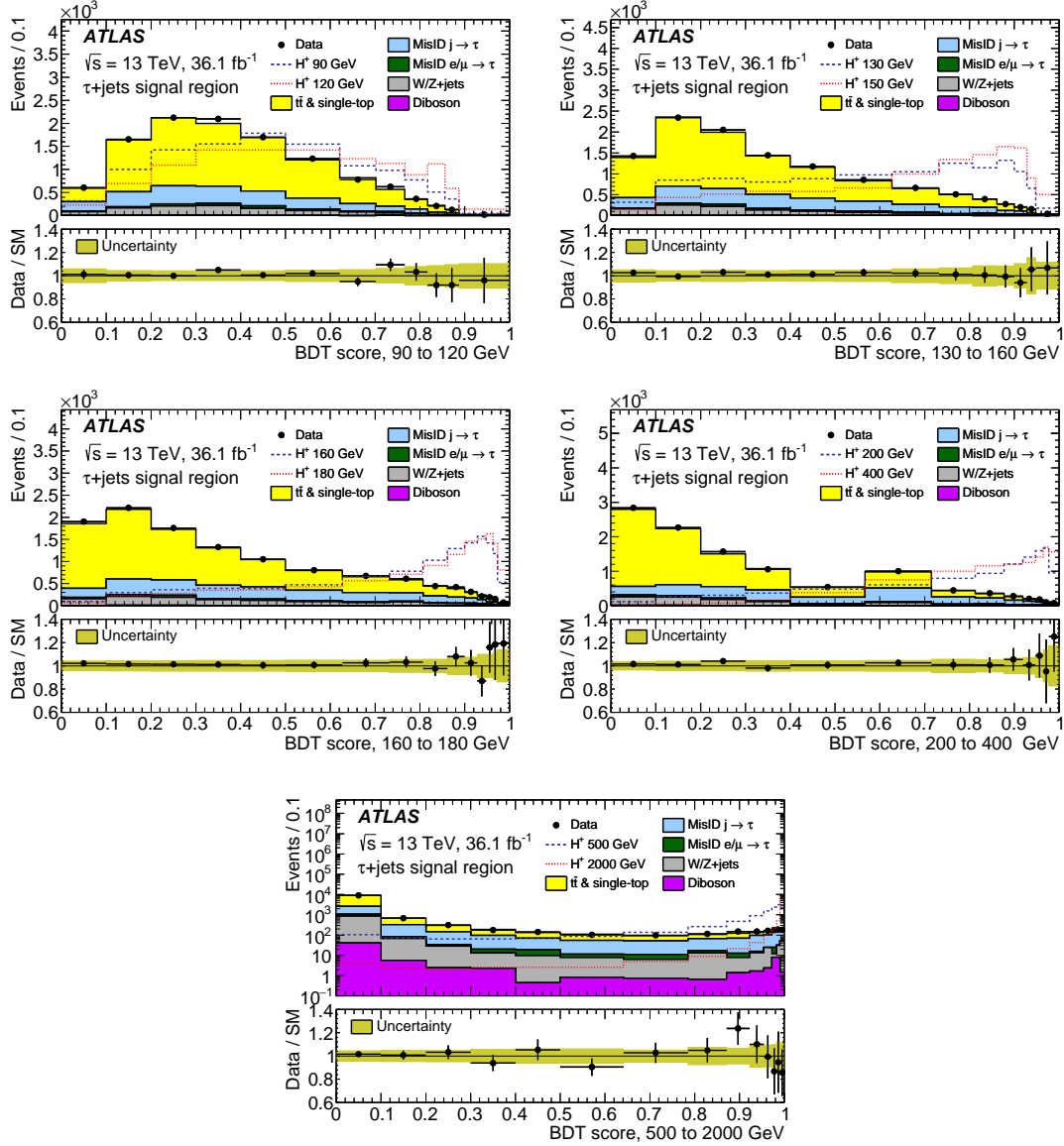


Figure 5: BDTs score distributions in the signal region of the  $\tau_h$ +jets channel, in the five mass ranges used for the BDTs trainings, after a fit to the data with the background-only hypothesis. The lower panel of each plot shows the ratio of data to the SM background prediction. The uncertainty bands include all statistical and systematic uncertainties. The normalisation of the signal (shown for illustration) corresponds to the integral of the background. [17]

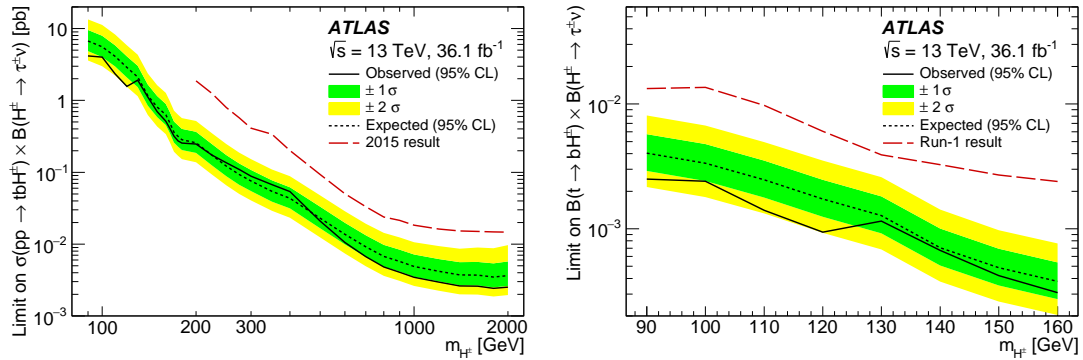


Figure 6: Observed and expected 95% CL on (left)  $\sigma(pp \rightarrow tbH^+) \times B(H^+ \rightarrow \tau\nu)$  and (right)  $B(t \rightarrow bH^+) \times B(H^+ \rightarrow \tau\nu)$  as a function of the charged Higgs boson mass, after combining the  $\tau_h$ +jets and  $\tau_h$ +leptons channels. [17]

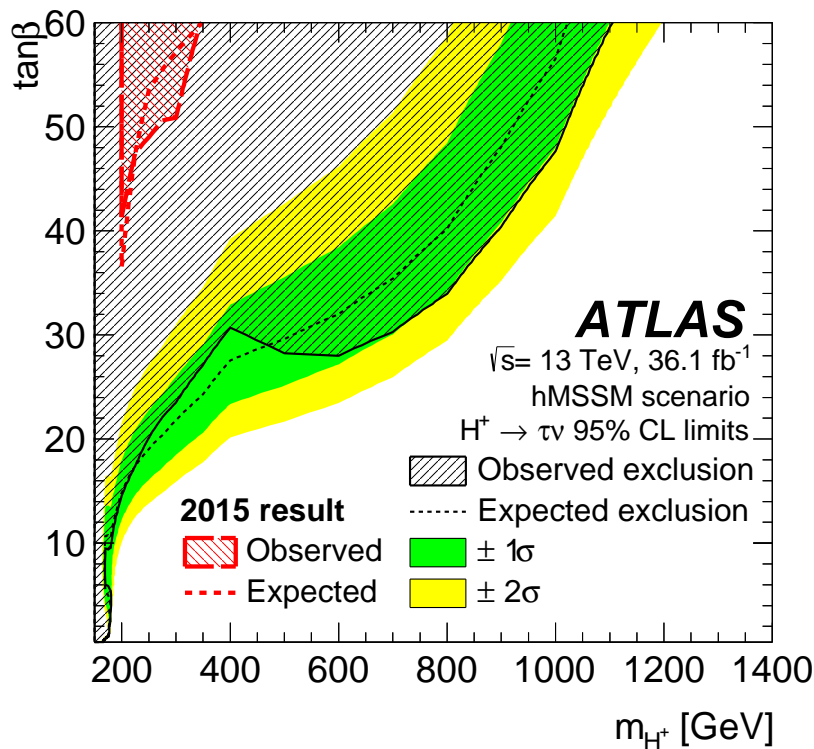


Figure 7: 95% CL exclusion limits on  $\tan\beta$  as a function of the charged Higgs boson mass in the context of the hMSSM scenario, for the regions in which theoretical predictions are available ( $0.5 \leq \tan\beta \leq 60$ ). [17]



## 145 4 Search for new light bosons in decays of the $h(125)$

146 The combination of data collected at center-of-mass energies of 7 and 8 TeV by ATLAS  
147 and CMS constrains branching fractions of the Higgs boson to particles beyond the SM  
148 to less than 34% at 95% CL [19]. Decay chain  $h(125) \rightarrow aa$  are allowed in 2HDM+S  
149 scenarios.

150 Four different type of 2HDM+S forbid flavour-changing neutral current at tree level.  
151 In Type-I, all SM particles couple to the first doublet. In Type-II, up-type quarks couple  
152 to the first doublet, whereas leptons and down-type quarks couple to the second doublet.  
153 NMSSM is a particular case of 2HDM+S of Type-II. In Type-III, quarks couple to the  
154 first doublet, and leptons to the second one. Finally, in Type-IV, leptons and up-type  
155 quarks couple to the first doublet, while down-type quarks couple to the second doublet.

156 The analysis here presented are based on pp collisions collected in 2016 by the CMS  
157 experiment at a center-of-mass energy of 13 TeV, corresponding to an integrated luminosity  
158 of  $35.9 fb^{-1}$ . Decay chains considered are  $aa \rightarrow b\bar{b}\tau\tau$  [20] and  $aa \rightarrow \mu\mu\tau\tau$  [21]. Masses of  
159 the pseudoscalar boson between 15.0 and 62.5 GeV are probed.

### 160 4.1 $h \rightarrow aa \rightarrow b\bar{b}\tau\tau$

161 Three different  $\tau\tau$  final states are considered:  $e\mu$ ,  $e\tau_h$ , and  $\mu\tau_h$ . They are additionally  
162 required to contain at least one b-tagged jet.

163 To increase the sensitivity of the analysis, events in each final state are separated into  
164 four categories with different signal-to-background ratios. The categories are defined on  
165 the basis of  $m_{\tau\tau b}^{vis}$ , the invariant mass of the visible decay products of the  $\tau$  leptons and  
166 the b-tagged jet with the highest  $p_T$ . This variable use the difference in the kinematic of  
167 the final objects in signal events and background events. Usually,  $m_{\tau\tau b}^{vis}$  has low values for  
168 the former and high for latter.

169 The dominant backgrounds, having these objects in the final state, are  $t\bar{t}$  and  $Z \rightarrow tt$   
170 production. Another large background consists of events with jets misidentified as  $\tau_h$ ,  
171 such as  $W$ +jets events, the background from SM events composed uniquely of jets pro-  
172 duced through the strong interaction, referred to as QCD multijet events, or semileptonic  
173  $tt$  events. The misidentified background is estimated through the *Fake Rate Method* de-  
174 scribed in [20].

### 175 4.2 $h \rightarrow aa \rightarrow \mu\mu\tau\tau$

176 The analysis focus on four different final states that cover the different possible  $\tau$  lepton  
177 decay modes:  $\mu\mu + e\mu$ ,  $\mu\mu + e\tau_h$ ,  $\mu\mu + \mu\tau_h$ , and  $\mu\mu + \tau_h\tau_h$ . The  $\mu\mu + ee$  and  $\mu\mu + \mu\mu$   
178 final states are not considered because of their smaller branching fractions and the large  
179 background contribution from ZZ production.

180 The background composed of events where at least one jet is misidentified as one of the  
181 final state leptons is estimated from data. Such events include mostly Z+jets and WZ+jets  
182 events, but there are also minor contributions from  $ZZ \rightarrow 2l2q$  events,  $t\bar{t}$  production, or  
183 from the background from SM QCD multijet events.

184 The analysis scans the reconstructed dimuon mass spectrum for a characteristic res-  
185 onance structure. The event selection and signal extraction used in this analysis are  
186 optimized for the  $h \rightarrow aa \rightarrow \mu\mu\tau\tau$  decay channel, where h has a mass of 125 GeV. Events  
187 from the  $h \rightarrow aa \rightarrow \tau\tau\tau\tau$  process can also enter the signal region when at least two of the  
188  $\tau$  leptons decay leptonically to muons and neutrinos. These events are treated as a part  
189 of the signal even if they do not exhibit a narrow dimuon mass peak.

### 190 4.3 Results

191 For the  $h \rightarrow aa \rightarrow bb\tau\tau$  decay channel, a global binned maximum-likelihood fit based  
 192 on the  $m_{\tau\tau}^{vis}$  distributions, in the different channels and categories, is performed for the  
 193 search for an excess of signal events over the expected background. Unbinned maximum-  
 194 likelihood fit to the dimuon invariant mass distribution is used in the  $h \rightarrow aa \rightarrow \mu\mu\tau\tau$   
 195 decay channel.

196 No significant excess of data is observed above the expected SM background. Upper  
 197 limits at 95% CL are set on  $(\sigma(h)/\sigma_{SM}) \times B(h \rightarrow aa \rightarrow \mu\mu\tau\tau)$  and  $(\sigma(h)/\sigma_{SM}) \times B(h \rightarrow$   
 198  $aa \rightarrow bb\tau\tau)$  for pseudoscalar masses between 15.0 and 62.5 GeV.

199 Figure 8 shows 95 % CL upper limits obtained from combining the different final state  
 200 considered in each analysis.

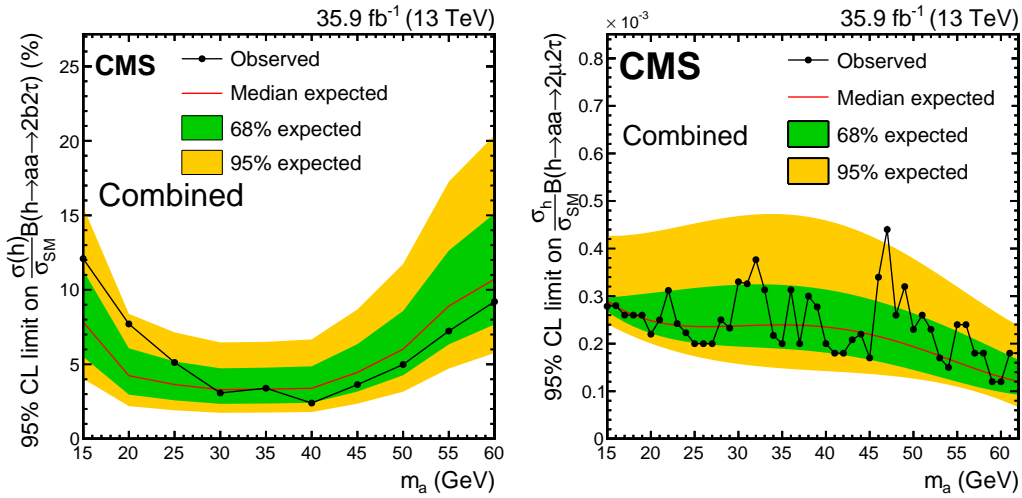


Figure 8: Upper limits at 95% CL on (left)  $(\sigma(h)/\sigma_{SM}) \times B(h \rightarrow aa \rightarrow bb\tau\tau)$  and on (right)  $(\sigma(h)/\sigma_{SM}) \times B(h \rightarrow aa \rightarrow \mu\mu\tau\tau)$  where the  $h \rightarrow aa \rightarrow 4\tau$  process is considered as a part of the signal, and is scaled with respect to the  $h \rightarrow aa \rightarrow \mu\mu\tau\tau$  signal. [20, 21]

201 This translates to limits on  $(\sigma(h)/\sigma_{SM}) \times B(h \rightarrow aa)$  in the different 2HDM+S sce-  
 202 narios. As explained at the beginning of Section 4.2, the different scenarios are related  
 203 to how the leptons, up-quark, and down-quark interact with the two doublets introduced.  
 204 The two analysis have different sensitivity in the  $m_a - \tan\beta$  plane due to the involvement  
 205 of down-quarks and leptons in the  $bb\tau\tau$  and only leptons in  $\mu\mu\tau\tau$ . In the Type-I scenario,  
 206 and Type-II scenario, with  $\tan\beta > 1$ , assuming the SM production cross section and  
 207 mechanisms for the Higgs boson, limits on  $(\sigma(h)/\sigma_{SM}) \times B(h \rightarrow aa)$  are about down to  
 208 20% for  $bb\tau\tau$  and down to 33% for  $\mu\mu\tau\tau$ . For Type-III and Type-IV scenarios, the limits  
 209 are depicted in Figure 9.

## 210 5 Conclusion

211 Several searches for BSM Higgs bosons, with tau leptons in the final state, have been  
 212 carried out in the ATLAS and CMS experiments using 2016 data at  $\sqrt{s} = 13$  TeV. No  
 213 evidence of additional Higgs bosons has been observed. Upper limits are provided on the  
 214 cross-section times branching fraction for different searches. The results are, furthermore,  
 215 interpreted in the context of an extended Higgs sector, such as MSSM and NMSSM. The  
 216 full Run-2 data, in which the integrated luminosity has reached  $\sim 140 fb^1$  will give an  
 217 incredible boost to the sensitivity for searches of new physics in the Higgs sector.

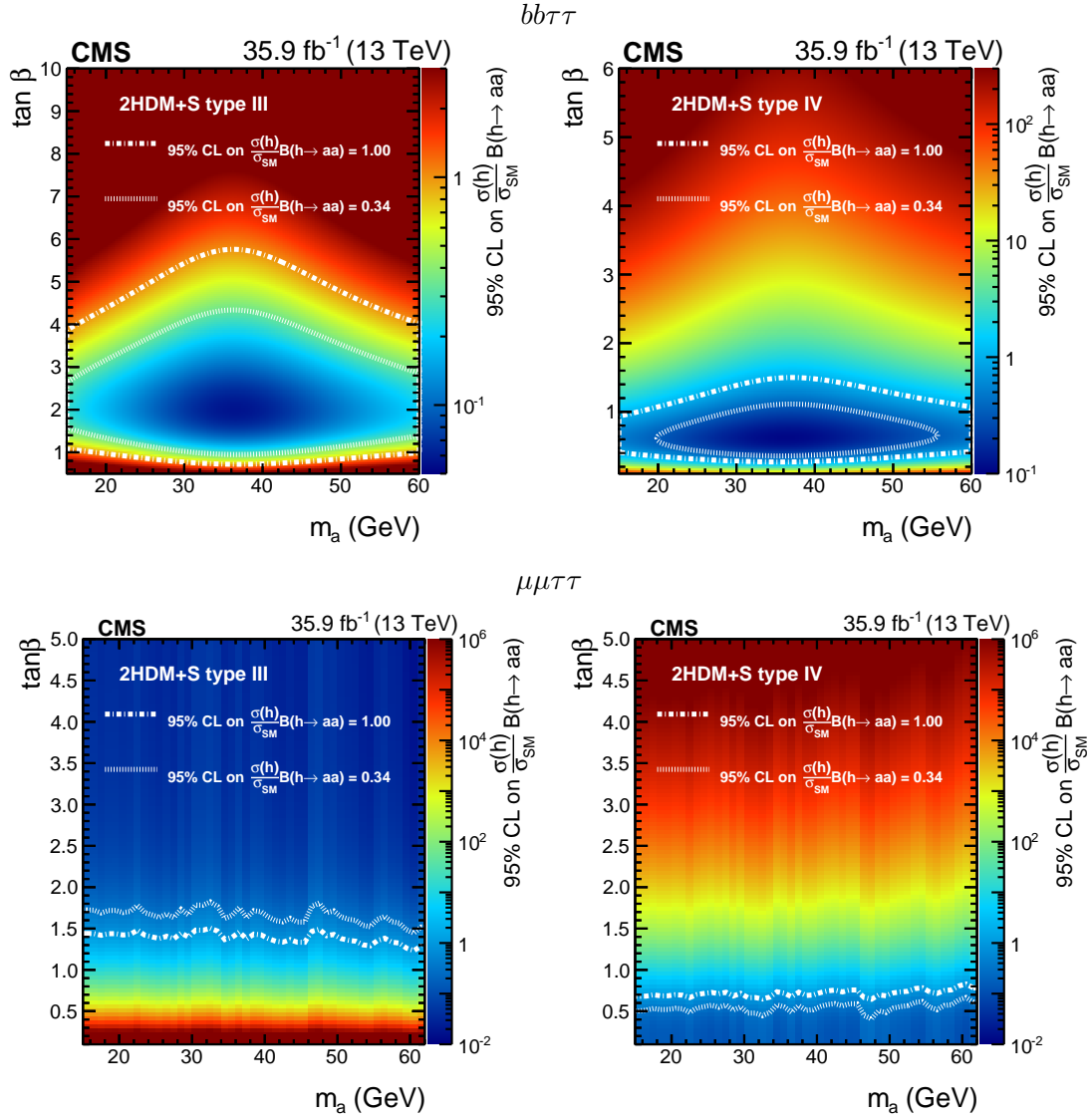


Figure 9: Observed 95% CL limits on  $(\sigma(h)/\sigma_{SM}) \times B(h \rightarrow aa)$  in 2HDM+S of type III (left), and type IV (right). The contours corresponding to a 95% CL exclusion of  $(\sigma(h)/\sigma_{SM}) \times B(h \rightarrow aa) = 1.00$  and  $0.34$  are drawn with dashed lines. The number 34% corresponds to the limit on the branching fraction of the Higgs boson to beyond-the-SM particles at the 95% CL obtained with data collected at center-of-mass energies of 7 and 8 TeV by the ATLAS and CMS experiments [19]. [20, 21]

## References

- 218
- 219 [1] G. Aad *et al.*, *The ATLAS Experiment at the CERN Large Hadron Collider*, JINST  
220 **3**, S08003 (2008), doi:10.1088/1748-0221/3/08/S08003.
- 221 [2] S. Chatrchyan *et al.*, *The CMS Experiment at the CERN LHC*, JINST **3**, S08004  
222 (2008), doi:10.1088/1748-0221/3/08/S08004.
- 223 [3] G. Aad *et al.*, *Observation of a new particle in the search for the Standard Model*  
224 *Higgs boson with the ATLAS detector at the LHC*, Phys. Lett. **B716**, 1 (2012),  
225 doi:10.1016/j.physletb.2012.08.020, 1207.7214.
- 226 [4] S. Chatrchyan *et al.*, *Observation of a new boson at a mass of 125*  
227 *GeV with the CMS experiment at the LHC*, Phys. Lett. **B716**, 30 (2012),  
228 doi:10.1016/j.physletb.2012.08.021, 1207.7235.
- 229 [5] S. Chatrchyan *et al.*, *Observation of a new boson with mass near 125 GeV in pp*  
230 *collisions at  $\sqrt{s} = 7$  and 8 TeV*, JHEP **06**, 081 (2013), doi:10.1007/JHEP06(2013)081,  
231 1303.4571.
- 232 [6] Yu. A. Golfand and E. P. Likhtman, *Extension of the Algebra of Poincare Group*  
233 *Generators and Violation of  $p$  Invariance*, JETP Lett. **13**, 323 (1971), [Pisma Zh.  
234 Eksp. Teor. Fiz.13,452(1971)].
- 235 [7] J. Wess and B. Zumino, *Supergauge Transformations in Four-Dimensions*, Nucl.  
236 Phys. **B70**, 39 (1974), doi:10.1016/0550-3213(74)90355-1, [24(1974)].
- 237 [8] P. Fayet, *Supergauge Invariant Extension of the Higgs Mechanism and a Model for*  
238 *the electron and Its Neutrino*, Nucl. Phys. **B90**, 104 (1975), doi:10.1016/0550-  
239 3213(75)90636-7.
- 240 [9] P. Fayet, *Spontaneously Broken Supersymmetric Theories of Weak, Electromag-*  
241 *netic and Strong Interactions*, Phys. Lett. **69B**, 489 (1977), doi:10.1016/0370-  
242 2693(77)90852-8.
- 243 [10] D. Curtin *et al.*, *Exotic decays of the 125 GeV Higgs boson*, Phys. Rev. **D90**(7),  
244 075004 (2014), doi:10.1103/PhysRevD.90.075004, 1312.4992.
- 245 [11] M. Aaboud *et al.*, *Search for additional heavy neutral Higgs and gauge bosons in the*  
246 *ditau final state produced in 36 fb<sup>1</sup> of pp collisions at  $\sqrt{s} = 13$  TeV with the ATLAS*  
247 *detector*, JHEP **01**, 055 (2018), doi:10.1007/JHEP01(2018)055, 1709.07242.
- 248 [12] A. M. Sirunyan *et al.*, *Search for additional neutral MSSM Higgs bosons in the*  
249  *$\tau\tau$  final state in proton-proton collisions at  $\sqrt{s} = 13$  TeV*, JHEP **09**, 007 (2018),  
250 doi:10.1007/JHEP09(2018)007, 1803.06553.
- 251 [13] H. S. S. O. e. a. Carena, M., *Mssm higgs boson searches at the lhc: benchmark*  
252 *scenarios after the discovery of a higgs-like particle*, Eur. Phys. J. C **73**, 2552 (2013),  
253 doi:10.1140/epjc/s10052-013-2552-1.
- 254 [14] D. de Florian *et al.*, *Handbook of LHC Higgs Cross Sections: 4. Deciphering the*  
255 *Nature of the Higgs Sector* (2016), doi:10.23731/CYRM-2017-002, 1610.07922.
- 256 [15] *Summary results of high mass BSM Higgs searches using CMS run-I data*, Tech. Rep.  
257 CMS-PAS-HIG-16-007, CERN, Geneva (2016).

- 258 [16] C. Degrande, R. Frederix, V. Hirschi, M. Ubiali, M. Wiesemann and M. Zaro, *Accu-*  
259 *rate predictions for charged Higgs production: Closing the  $m_{H^\pm} \sim m_t$  window*, Phys.  
260 Lett. **B772**, 87 (2017), doi:10.1016/j.physletb.2017.06.037, 1607.05291.
- 261 [17] M. Aaboud *et al.*, *Search for charged Higgs bosons decaying via  $H^\pm \rightarrow$*   
262  *$\tau^\pm \nu_\tau$  in the  $\tau$ +jets and  $\tau$ +lepton final states with  $36 \text{ fb}^{-1}$  of  $pp$  collision data*  
263 *recorded at  $\sqrt{s} = 13 \text{ TeV}$  with the ATLAS experiment*, JHEP **09**, 139 (2018),  
264 doi:10.1007/JHEP09(2018)139, 1807.07915.
- 265 [18] C. Collaboration, *Search for charged Higgs bosons with the  $H^\pm \rightarrow \tau^\pm \nu_\tau$  decay channel*  
266 *in proton-proton collisions at  $\sqrt{s} = 13 \text{ TeV}$*  (2018).
- 267 [19] G. Aad *et al.*, *Measurements of the Higgs boson production and decay rates*  
268 *and constraints on its couplings from a combined ATLAS and CMS analysis of*  
269 *the LHC  $pp$  collision data at  $\sqrt{s} = 7$  and  $8 \text{ TeV}$* , JHEP **08**, 045 (2016),  
270 doi:10.1007/JHEP08(2016)045, 1606.02266.
- 271 [20] A. M. Sirunyan *et al.*, *Search for an exotic decay of the Higgs boson to a*  
272 *pair of light pseudoscalars in the final state with two  $b$  quarks and two  $\tau$  lep-*  
273 *tons in proton-proton collisions at  $\sqrt{s} = 13 \text{ TeV}$* , Phys. Lett. **B785**, 462 (2018),  
274 doi:10.1016/j.physletb.2018.08.057, 1805.10191.
- 275 [21] A. M. Sirunyan *et al.*, *Search for an exotic decay of the Higgs boson to a pair of*  
276 *light pseudoscalars in the final state of two muons and two  $\tau$  leptons in proton-proton*  
277 *collisions at  $\sqrt{s} = 13 \text{ TeV}$*  (2018), 1805.04865.